VIP Antibiotic Biosynthesis

DOI: 10.1002/anie.201108896

The *O*-Carbamoyltransferase TobZ Catalyzes an Ancient Enzymatic Reaction**

*Christoph Parthier, Stefan Görlich, Frank Jaenecke, Constanze Breithaupt, Ulrike Bräuer, Uwe Fandrich, Diana Clausnitzer, Udo F. Wehmeier, Christoph Böttcher, Dierk Scheel, and Milton T. Stubbs**

Dedicated to Professor Robert Huber on the occasion of his 75th birthday and to Professor Wolfram Bode on the occasion of his 70th birthday

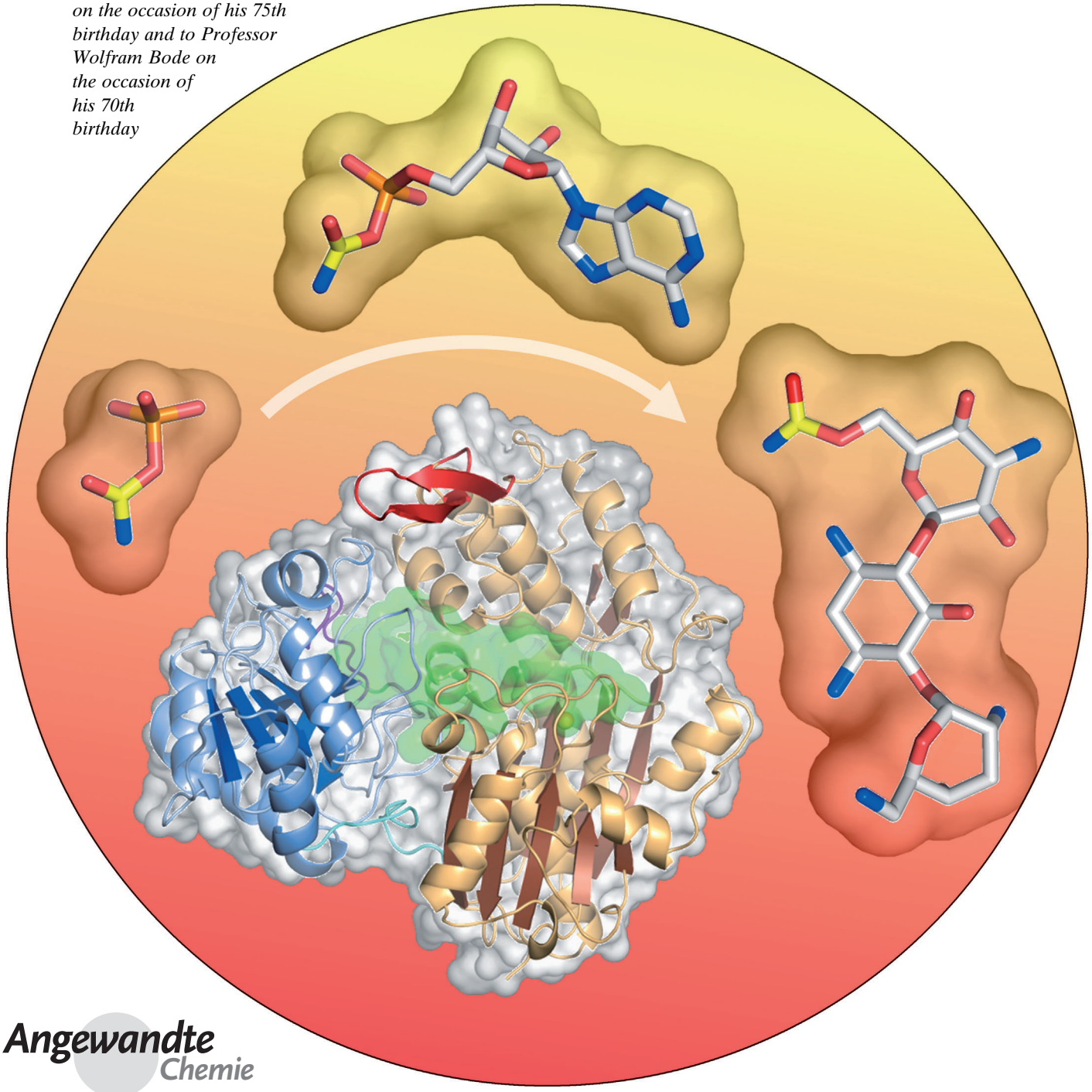

The biosynthetic modification of secondary metabolites is responsible for the immense diversity of natural products, and allows for their pharmaceutical application in the form of, for example, antibiotic, antiviral, and anticancer agents.[1] Whereas tailoring reactions such as glycosylation and prenylation have been characterized extensively both functionally and structurally, the nature of the *O*-carbamoylation reaction (transfer of a carbamoyl group to a substrate hydroxy function) is so far unclear. *O*-Carbamoylation has been observed in a variety of secondary metabolites, including antibiotics as diverse as cephalomycin,[2] novobiocin,[3] and nebramycin,[4,5] as well as rhizobial nodulation (Nod) factors[6] (responsible for legume host specificity) and saxitoxin[7] (the causative agent of paralytic shellfish poisoning). As with the aspartate and ornithine *N*-carbamoyltransferases (CTases) of primary metabolism, the source of the carbamoyl moiety is the energy-rich substrate carbamoylphosphate (**1**, Figure 1 B); in contrast to the latter enzymes, however, early studies on the biosynthesis of the β-lactam antibiotic cephamycin[2] showed that the enzyme involved, carbamoylphosphate-3-hydroxymethylcephem *O*-CTase (CmcH), is stimulated by the presence of ATP. Sequence comparisons with the rhizobial enzyme NodU, responsible for the *O*-carbamoylation of Nod factor,[6] showed that the two proteins belong to a broader class of enzymes, designated CmcH/NodU CTases.[8] In vitro studies on the *O*-CTase NovN, involved in the biosynthesis of the bacterial DNA gyrase inhibitor novobiocin, confirmed the intriguing Mg^{2+}-ATP dependency observed for CmcH.[3]

Tobramycin (**3**), an aminoglycoside closely related to kanamycin and gentamicin, exerts its antibiotic effects through binding to a deep groove in the aminoacyl decoding site of 16S ribosomal RNA.[9] Genetic analysis of the tobramycin gene cluster from *Streptoalloteichus tenebrarius*[5] indicated the presence of a putative *O*-CTase TobZ (also termed TacA[4]), and the heterologously produced protein exhibits ATP-dependent carbamoylation of both **3** and kanamycin A to form nebramycin 5′ (**4**) and the new product

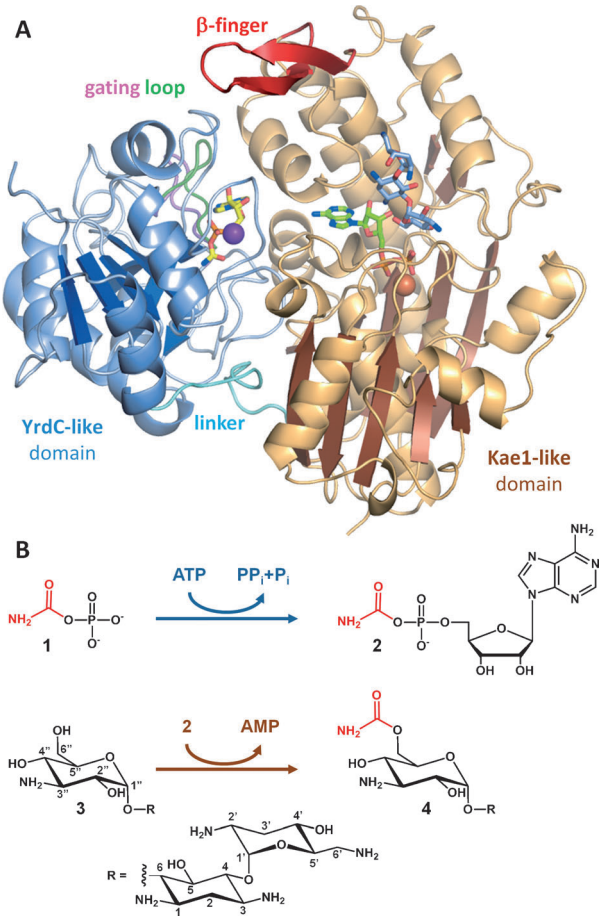

Figure 1. A) The Kae1-like ASKHA (brown, red) and YrdC-like (blue) domains of TobZ with selected substrates and intermediates. Orange: bound iron atom; magenta: Mg^{2+}/Mn^{2+}; yellow: YrdC-site carbamoyladenylate (**2**); green: Kae1-site ADP; light blue: tobramycin (**3**). Nucleotide occupation of the YrdC-site results in closure of the gating loop (pink: "open"; green: "closed"). B) Reactions catalyzed by TobZ.

carbamoyl-kanamycin A respectively (Figure S1 in the Supporting Information). Here we provide evidence that TobZ catalyzes a two-step reaction involving a carbamoyladenylate intermediate (**2**), and that adenylate synthesis and carbamoyl transfer take place at separate active sites. Domain conservation, functional similarities, and re-evaluation of published structural data suggest that analogous reactions occur in the maturation of [NiFe]-hydrogenase and in the synthesis of the essential tRNA modification threonylcarbamoyladenosine.

TobZ possesses two major domains (Figure 1 A), with the larger domain (M1–A354) belonging to the ASKHA (acetate and sugar kinases, Hsc70, actin) superfamily[10] and consisting of two similar α/β subdomains with an additional protruding two-stranded β-sheet "finger" (E251–R269). Interestingly, the region corresponding to the ATP-binding site of these enzymes contains an iron (or zinc) atom, coordinated by TobZ residues H114, H118, D137, and D338 that (with the exception of D137) are conserved in other CmcH/NodU CTases (Figure S2 in the Supporting Information). Until now, the only other member of the ASKHA superfamily shown to bind metal (also iron) is the universal protein Kae1 (kinase-associated endopeptidase 1),[11,12] and indeed the putative

[*] Dr. C. Parthier,[+] S. Görlich,[+] F. Jaenecke, Dr. C. Breithaupt, U. Bräuer, U. Fandrich, Prof. Dr. M. T. Stubbs
Institut für Biochemie und Biotechnologie
Martin-Luther-Universität Halle-Wittenberg
Kurt-Mothes-Strasse 3, 06120 Halle (Saale) (Germany)
E-mail: stubbs@biochemtech.uni-halle.de
Dr. D. Clausnitzer, Priv.-Doz. Dr. U. F. Wehmeier
Chemische Mikrobiologie/Lehrstuhl für Sportmedizin
Bergische Universität Wuppertal
42097 Wuppertal (Germany)
Dr. C. Böttcher, Prof. Dr. D. Scheel
Leibniz-Institut für Pflanzenbiochemie
Weinberg 3, 06120 Halle (Saale) (Germany)
[+] These authors contributed equally to this work.
[**] This work was supported in part by the DFG Schwerpunktprogramm SPP1152 "Evolution metabolischer Diversität" and the Landesexzellenzinitiative Sachsen-Anhalt "Strukturen und Mechanismen der biologischen Informationsverarbeitung" (M.T.S.) as well as by the "GenoMik-plus" program of the BMBF (D.C. and U.F.W.).
Supporting information for this article is available on the WWW under http://dx.doi.org/10.1002/anie.201108896.

active sites of the two structures are highly similar. The smaller domain (D367–H570) consists of a highly twisted, open α/β sheet, and exhibits significant structural homology to members of another universal protein family, YrdC/Sua5 (suppressor of upstream ATG).[13–15] Juxtaposition of the two domains results in a spacious internal cavity (Figure S3 in the Supporting Information), with an opening above the iron site that could be closed completely by adjustment of the β-sheet "finger". Between the two domains, a tartrate ion from the crystallization buffer is found, surrounded by a high local concentration of basic groups (Figure S4 A in the Supporting Information).

Introduction of **1** into the crystals of TobZ displaces the tartrate ion, revealing the binding site for **1** to be at the interface between the two domains (Figure S4 B; see Figure 1) some 20 Å away from the iron binding site. The carboxamide group of **1** is held in place by four hydrogen bonds to the backbone atoms A419^{N}, A419^{O}, and N528^{O} and the guanidinyl group of R418, whereas its phosphate moiety is coordinated by side-chain atoms of R498$^{N\eta1/N\eta2}$, T529$^{O\gamma1}$, and S530$^{O\gamma}$ as well as the backbone amide nitrogen S530^{N}. No significant structural rearrangements are observed upon binding of **1**, apart from a reorientation of the arginine side chains R418 and R498. All residues involved in binding of **1** are absolutely conserved in *O*-CTases (Figure S2 in the Supporting Information).

No difference electron density was observed for TobZ crystals soaked with ATP analogues; on the other hand, in the presence of ADP, the nucleotide was detected at the subdomain interface of the Kae1-like domain, with the iron atom coordinating both α- and β-phosphates (Figure 1 and Figure S5 A in the Supporting Information). The β-phosphate exhibits the largest number of contacts: in addition to the bond to iron, it is within hydrogen-bonding distance of the iron ligands H114 and D338 as well as the backbone amides of G138 and Q139 and the imidazole function of H14. The α-phosphate contacts the iron ligands H118 and D338 in addition to the backbone amides of G310 and D338, and the ribose hydroxy groups make hydrogen bonds to G168^{O} and E172$^{O\varepsilon1}$. The adenine base stacks against the Y171 side chain, which forms one wall of a pocket delineated by P185, G186, M189, V311, and L313; a single hydrogen bond is observed between the ADP N1 nitrogen and N314$^{O\delta1}$. Only minor rearrangements are associated with nucleotide binding: the protein–iron coordination changes from a bidentate D137 side-chain interaction to a monodentate one, and the side chain of E172 adjusts to accommodate the ribose moiety.

Simultaneous soaking of TobZ crystals with **1** and ATP resulted in additional difference electron density in the YrdC-like domain clearly interpretable as carbamoyladenylate (**2**; Figures 1 B and 2 A, and Figure S4 D in the Supporting Information). The adenine base is accommodated in a broad pocket that is inaccessible to bulk solvent through closure of the conserved surface loop V490–R498 (which we have termed the "gating loop"), and exhibits only few close contacts to the protein: some near-stacking arrangements of the base to the side chains of P450 as well as H492 and R498 of the gating loop, together with a hydrogen bond between ribose O3′ and R449$^{N\eta2}$. The phosphate moiety of the adenylate is superimposable on that of **1**, with a shift of main-chain segment D533–E536 and the guanidinium group of R445 from their positions in the **1**-bound structure. Moreover, a second molecule of **2** substitutes for the ADP molecule observed previously in the iron binding site (Figure 2 B and Figure S5 B in the Supporting Information), with the carboxamide nitrogen held in position by the iron atom, D338$^{O\delta2}$, and the Q139 backbone carbonyl oxygen, and the oxygen atom approaching the backbone amides of G138 and Q139.

TobZ crystals soaked with **1**, the ATP analogue AMPCPP, and manganese confirmed the nucleotide binding site in the YrdC-like domain (Figure 2 C and Figure S4 C in the Supporting Information), with no electron density at the iron site. The positions of the adenine and ribose moieties shift from those observed in the complex with **2** (with the ribose C4′ moving some 2.3 Å), accompanied by minor side-chain

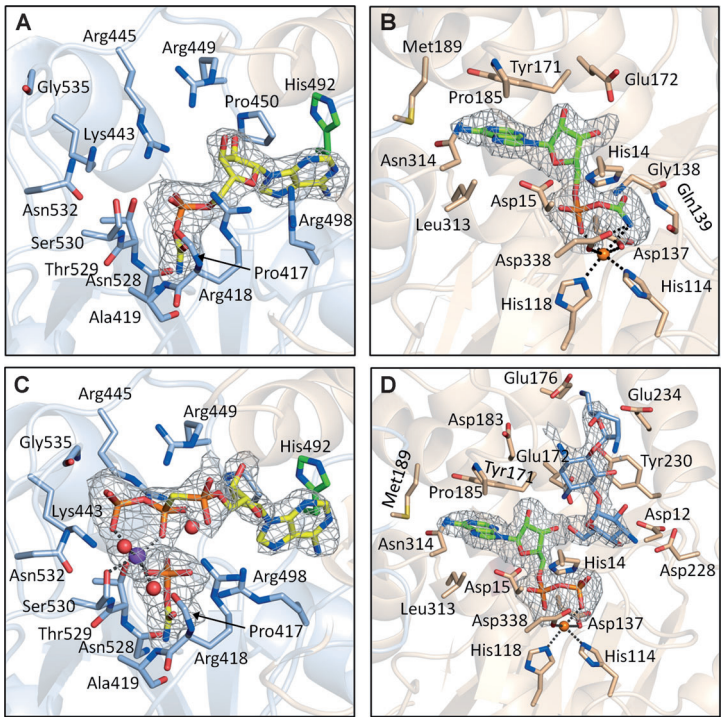

Figure 2. A) The intermediate carbamoyladenylate (**2**) is observed at the YrdC domain in crystals of TobZ soaked with **1**, ATP, and Mn^{2+}. Nucleotide binding results in closure of the H492-containing gating loop. B) **2** is found in the same crystal at the Kae1-domain, where the carboxamide moiety contacts the iron atom and juxtaposes the backbone amides of G138 and Q139. C) Soaking TobZ crystals with AMPCPP, **1**, and Mn^{2+} results in clear density for each component, revealing octahedral coordination of the cation (magenta) and ordered solvent molecules (red spheres). D) At the Kae1-like site, tobramycin and ADP are found upon soaking with the antibiotic, **1**, and ADP. The aminoglycoside is bound for the most part by electrostatic interactions, with the 6″-hydroxy acceptor group in the neighborhood of H^{14} and the ADP β-phosphate. F_o-F_c electron density maps are contoured at 3 σ.

rearrangements of the side chains of R498 and R445. The majority of enzyme–nucleotide interactions are contributed by the phosphate moieties. The γ-phosphate is held in place by interactions with the side chains of $K443^{N\zeta}$, $R445^{N\eta1}$, $S530^{O\gamma}$, and $N532^{N\delta2}$ as well as the backbone amide $G535^{N}$. The nucleotide β-phosphate contacts $R449^{N\eta2}$ as well as $R418^{N\eta2}$, which also interacts with both the AMPCPP α- and the **1**-phosphates. Notably, an octahedrally coordinated Mn^{2+} ion accompanies AMPCPP binding, with equatorial ligands β-/γ-phosphate $AMPCPP^{O2\beta/O2\gamma}$, $S530^{O\gamma}$, and a solvent molecule (ligated in turn by $P417^{O}$ and the **1** carboxamide oxygen), and axial ligands $\mathbf{1}^{O1P}$ and a second solvent molecule. Completing the nucleotide binding site, a third solvent molecule is found within hydrogen-bonding distance of the β-phosphate $AMPCPP^{O1\beta}$, the ribose O2' atom, and $R445^{N\eta2}$. Mutations in this region (Supporting Information) provide confirmation that the YrdC-like domain, with a cryptic **1**-dependent Mg^{2+}-ATP binding site, is responsible for synthesis of **2**.

The binding site for the aminoglycoside could be delineated in crystals soaked with **1**, ADP, and **3** (Figure 2D). The central 2-deoxystreptamine moiety of the antibiotic stacks over the side chain of Y^{230}, whereas the basic amino groups juxtapose the carboxylate groups of D12, D183, E172, E176, D228, and E234. The 6″-hydroxy group of the substrate approaches H14 and the iron-bound α- and β-phosphates of the nucleotide, indicating that this is the site for carbamoyl transfer.

To gain further insights into the reaction, we followed catalysis using α- and γ-^{32}P-labeled ATP (Figure S7 in the Supporting Information). Reactions carried out in the presence of **1**, **3**, and α-^{32}P-ATP resulted in the exclusive production of labeled AMP. Utilization of γ-^{32}P-ATP produced radioactive pyrophosphate only, suggesting that TobZ catalyzes an ATP-pyrophosphatase reaction, confirmed by the dependency of the ATP-$^{32}PP_i$ pyrophosphate exchange reaction on **1**. Presumably, ATP-pyrophosphatase activity is accompanied by **1**-phosphate cleavage to yield the intermediate **2** and ultimately AMP. Having observed the presence of ADP bound to the Kae1-like site, as well as a solvent-mediated contact between the ATP 2′-hydroxy group and the β-phosphate in the **1**-AMPCPP complex, we tested the effect of other nucleotides on the carbamoylation reaction (Figure S9 in the Supporting Information). We found that ADP inhibits the formation of **4**, and that the reaction is considerably slower in the presence of deoxy-ATP.

Combining the structural and biochemical data presented here, we propose a reaction sequence for TobZ as outlined in Figure 3. Binding of **1** within a narrow cavity at the base of the reaction chamber completes an otherwise cryptic secondary binding site for Mg^{2+}-ATP, which upon binding causes closure of the gating loop. Salt-bridge formation between Mg^{2+} and one of the **1** phosphate oxygens would enhance the electrophilicity of the **1**-phosphorus and stabilize the developing negative charge during hydrolysis. We suggest that a water molecule could occupy the free space between **1** and the ATP β-phosphate opposite to the scissile bond of **1**, to be activated for nucleophilic attack through deprotonation either by one of the ATP β-phosphate oxygens (in analogy to nucleophile activation by one-metal-ion type II restriction enonucleases[16]) or by means of an hydroxide ion coordinated to Mg^{2+} (as discussed for self-splicing of the hammerhead ribozyme[17]). Following hydrolysis, both products remain trapped in the cavity because of the presence of the ATP molecule, thereby protecting the reactive carbamate. The ensuing adenylation reaction could be initiated by a shift of the ATP ribose and α-phosphate moieties to their positions observed in the **2** complex structure; displacement of the cleaved phosphate by the ATP α-phosphate would position the latter for in-line nucleophilic attack of carbamate and release of pyrophosphate. It is worthy of note that the protein seems to play a solely passive role in the adenylation reaction: all functional groups appear to be provided by the substrates themselves, representing an extreme form of substrate-assisted catalysis.

Coupling of pyrophosphate/phosphate release to side-chain rearrangements of the numerous basic groups in the neighborhood, as has been proposed for adenylation domains of nonribosomal peptide synthetases (NRPSs),[18] could provide a driving force for translocation of the intermediate **2** from its site of formation to the carbamoyltransfer domain along the electrostatic potential gradient within the "reaction chamber" (Figure S3 in the Supporting Information). Upon arrival at the carbamoyl-transfer site, a close approach of the tobramycin (**3**) 6″-hydroxy group to the active site would allow proton abstraction by the H14/D15 dyad, facilitating nucleophilic attack at the carbamoyl group to result in a tetrahedral intermediate (mimicked by the ADP molecule at the iron site) whose oxyanion would be stabilized by the backbone amides $G138^{N}$/$Q139^{N}$ (Figure 3B,C). Departure of the AMP leaving group would then lead to the formation of the product nebramycin 5′ (**4**). It should be noted, however, that both the precise nature and role of the metal ion in catalysis remain unclear at present.

Strong sequence conservation within the CmcH/NodU family (Figure S2 in the Supporting Information) implies that this mechanism is relevant to the other known secondary metabolite *O*-CTases. Thus, the TobZ/CmcH/NodU *O*-CTases constitute a novel class of the adenylate-forming enzyme superfamily (reviewed in reference [19]) that includes aminoacyl-tRNA synthetases, the adenylation domains of nonribosomal peptide synthetases (NRPSs), and the NRPS-independent siderophore synthetases as well as the ubiquitin-activating E1 enzymes, with one important distinction: all these enzymes activate a substrate carboxylate group by means of pyrophosphate hydrolysis, whereas the TobZ/CmcH/NodU *O*-CTases perform an additional phosphate cleavage of **1**. But why sacrifice a phosphate anhydride at the expense of ATP? The answer may lie in the fact that carbamate decomposes readily to form carbon dioxide and ammonia; coupling to phosphate in **1** or to AMP in **2** provides protection for the labile intermediate, allowing transport between active sites. Various mechanisms may serve to direct this seemingly profligate use of energy-rich substrates: 1) Mg^{2+}-ATP binds to the secondary binding site only in the presence of cosubstrate **1**; 2) occupation of the adenylation site results in closure of the gating loop, restricting diffusion of substrates; 3) removal of magnesium/phosphate/pyrophos-

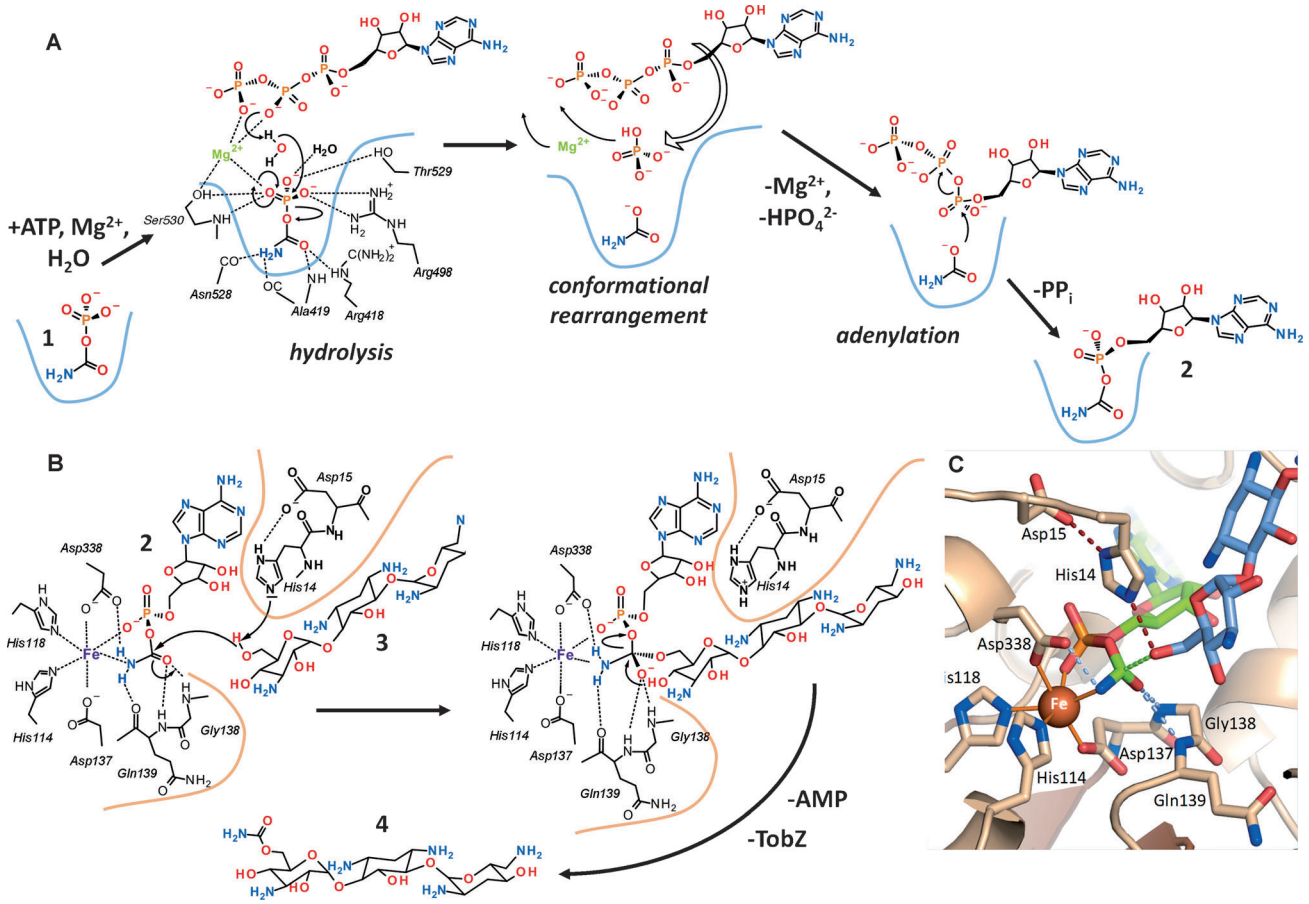

Figure 3. TobZ catalyzes two half-reactions (see text and the Supporting Information for details). A) The first half-reaction, hydrolysis of **1** and subsequent adenylation by ATP to form **2**, is catalyzed by the YrdC-like domain. B) The Kae1-like domain catalyzes transfer of the carbamoyl moiety from **2** to the tobramycin (**3**) 6″-hydroxy group. C) Proposed transition state for the transfer reaction.

phate (facilitated by the electrostatic distribution within the chamber) can drive the reaction in favor of adenylate formation; and 4) the observed inhibition by ADP could restrict unproductive ATP hydrolysis.

Consecutive fused YrdC-like and Kae1-like modules are also found in the [NiFe]-hydrogenase maturation factor HypF,[20] although the order of the domains is reversed compared to TobZ. HypF catalyzes the carbamoylation of the C-terminal cysteine residue of HypE in a key step of [NiFe]-hydrogenase complex biosynthesis,[21,22] which in turn is essential for the reversible catalysis of dihydrogen into protons and electrons in archaea, many anaerobic bacteria as well as some lower eukarya.[23] Like TobZ, HypF exhibits ATP-dependent CTase activity, where the carbamoyl moiety is also derived from carbamoylphosphate **1**, and the intermediate **2** has been postulated.[20,24,25] It is therefore likely that HypF catalysis involves corresponding reactions to those described for TobZ.

The conserved universal proteins YrdC/Sua5 and Kae1 have been shown recently to be involved in the biosynthesis of the modified tRNA base threonylcarbamoyladenosine (t^6A_{37}).[26–29] The modification is essential for correct decoding by the ribosome,[30] explaining a wide range of pleiotropic effects observed as a result of Sua5/Kae1 mutations (including various growth defects and telomere dysfunction, reviewed in references [26–28]). Earlier structural genomics studies on YrdC/Sua5 showed them to possess adenine nucleotide and nucleic acid binding properties.[13,15] The TobZ adenylation site is highly similar to the nucleotide-binding site identified in the YrdC domain of Sua5, with conservation of residues corresponding to K57/R59/P64 in Sua5 and K443/R445/P450 in TobZ (Figure S10 in the Supporting Information). The binding sites also reveal significant preservation of contacts identified in TobZ as being important for carbamoylphosphate binding; in particular, the main-chain atoms of TobZ N528-T529-S530 as well as the side-chain hydroxy atoms are positioned equivalently to those of the corresponding residues in YrdC (S137-T138-S139) and Sua5 (A142-P143-S144). The loop insertion containing the highly conserved GPRAL sequence of the secondary metabolite *O*-CTases (in TobZ positions 416–420, of which the A419 backbone atoms make dual hydrogen bonds to the carbamoylphosphate carboxamide), is, however, conspicuously absent in YrdC and Sua5.

Identification of **2** in the crystal structure of TobZ prompted us to re-examine the published crystallographic data for Sua5 from *Sulfolobus tokadaii*.[13] Unbiased difference electron density shows clearly the presence of threonylcarbamoyladenylate in the putative active site of Sua5

(Figure S10 in the Supporting Information), derived presumably from the *E. coli* expression host and interpreted previously in the form of AMP and solvent molecules.[13] As observed recently for Sua5 in complex with L-threonine and AMPPNP,[31] the threonyl moiety occupies a small pocket (not present in TobZ) and is coordinated by multiple interactions: the side-chain hydroxy group makes hydrogen bonds to $H68^{N\varepsilon 2}$ and $R122^{N\varepsilon}$ (which in turn is involved in a salt bridge with E35), while the free terminal carboxylic acid hydrogen bonds to $T36^{O\gamma 1}$, $S182^{N/O\gamma}$, and $R196^{N\eta 2}$. $R196^{N\eta 2}$ is also hydrogen-bonded to $S182^{O}$ and the phosphate O1 of the adenylate, interactions that are also observed in TobZ (where the R418 guanidinium group of the GPRAL sequence coordinates binding of the adenylate phosphate) and could also be fulfilled in YrdC by R188.

Thus the bona fide YrdC domain can bind and protect the threonylcarbamoyladenylate intermediate. Biosynthesis of t^6A_{37} requires threonine, bicarbonate, and ATP, with hydrolysis of at least two ATP molecules,[32,33] and it has been proposed that bicarbonate is activated by ATP to yield carboxyphosphate and ADP. Reaction of carboxyphosphate with threonine could then produce *N*-carboxythreonine as the starting point for t^6A_{37} synthesis. Kuratani et al.[31] have hypothesized that YrdC/Sua5 might catalyze *N*-carboxythreonine synthesis; this seems unlikely, as there is neither sufficient space between threonine and AMPPNP for bicarbonate binding, nor is AMPPNP (ATP) positioned correctly for γ-phosphate transfer. Our data suggest that YrdC/Sua5 catalyzes a "classical" adenylation reaction (R-COOH + ATP→R-C=O-AMP + PP_i) of *N*-carboxythreonine and ATP to form the threonylcarbamoyladenylate intermediate, analogous to the carbamate adenylation step proposed here for TobZ (Figure 3A). Indeed, a corresponding YrdC-catalyzed adenylation reaction has recently been put forward by El Yacoubi and co-workers,[27] who further attribute to YrdC the transfer of threonylcarbamoyl to tRNA and assign the function of Kae1 to *N*-carboxythreonine synthesis. Considering the strong resemblance of the active site of Kae1[11] to the CTase domain in TobZ, however, in which not only the iron- and ATP-binding sites are similar, but also the putative oxyanion hole formed by the backbone amides of G138 and Q139 in TobZ and G130 and G131 in Kae1 is conserved (Figures S11 and S12 in the Supporting Information), we advocate that Kae1 is responsible for threonylcarbamoyl transfer to yield t^6A_{37}. The present data and the observation that in vitro t^6A_{37} synthesis requires the presence of cell extracts in addition to purified YrdC/Sua5 and Kae1[27,28] make it probable that *N*-carboxythreonine is generated from bicarbonate and threonine by an as yet unknown enzymatic activity.

Thus, TobZ is representative of an ancient modular enzyme family, members of which are responsible for crucial biosynthetic reactions in [NiFe]-hydrogenase maturation[25] and in the formation of the universal tRNA modification threonylcarbamoyladenosine.[26–28] The presumed ancient origin of the reaction suggests a further reason for the puzzling and seemingly wasteful use of **1** and ATP: being functional for an essential biotic reaction (t^6A_{37} biosynthesis), the responsible enzymes have withstood evolutionary selective pressure, providing a blueprint for alternative uses in later evolution such as antibiotic synthesis. Division of labor—ATP-dependent carbamoyl adenylation and carbamoyl transfer—between the modules, as well as the fundamental enzymatic reactions, appear to have been conserved from early in evolution to the present day. Streptomycetes (producers of nebramycin, cephamycin, novobiocin), rhizobia (nodulation factors), and cyanobacteria (saxitoxin) appear to have co-opted two modules of this Ur-enzyme, fusing them for the production of secondary metabolites. The inherent safety mechanisms essential for primordial metabolic processes—regulated use of substrates carbamoylphosphate and ATP, as well as sequestration of intermediates—might allow present-day organisms to adapt secondary metabolite repertoires (e.g. nebramycin or tobramycin production) to the prevailing metabolic state.

Received: December 17, 2011
Published online: March 1, 2012

Keywords: antibiotics · biosynthesis · evolution · RNA · structural biology

[1] C. T. Walsh, M. A. Fischbach, *J. Am. Chem. Soc.* **2010**, *132*, 2469–2493.
[2] S. J. Brewer, P. M. Taylor, M. K. Turner, *Biochem. J.* **1980**, *185*, 555–564.
[3] C. L. Freel Meyers, M. Oberthur, H. Xu, L. Heide, D. Kahne, C. T. Walsh, *Angew. Chem.* **2004**, *116*, 69–72; *Angew. Chem. Int. Ed.* **2004**, *43*, 67–70.
[4] M. K. Kharel, D. B. Basnet, H. C. Lee, K. Liou, J. S. Woo, B. G. Kim, J. K. Sohng, *Fems Microbiol. Lett.* **2004**, *230*, 185–190.
[5] U. F. Wehmeier, W. Piepersberg, *Methods Enzymol.* **2009**, *459*, 459–491.
[6] S. Jabbouri, R. Fellay, F. Talmont, P. Kamalaprija, U. Burger, B. Relic, J. C. Prome, W. J. Broughton, *J. Biol. Chem.* **1995**, *270*, 22968–22973.
[7] R. Kellmann, T. K. Michali, B. A. Neilan, *J. Mol. Evol.* **2008**, *67*, 526–538.
[8] J. J. R. Coque, F. J. Perezllarena, F. J. Enguita, J. L. Fuente, J. F. Martin, P. Liras, *Gene* **1995**, *162*, 21–27.
[9] Q. Vicens, E. Westhof, *Chem. Biol.* **2002**, *9*, 747–755.
[10] J. H. Hurley, *Annu. Rev. Biophys. Biomol. Struct.* **1996**, *25*, 137–162.
[11] A. Hecker et al., *Nucleic Acids Res.* **2007**, *35*, 6042–6051.
[12] D. Y. L. Mao et al., *Mol. Cell* **2008**, *32*, 259–275.
[13] Y. Agari, S. Sato, T. Wakamatsu, Y. Bessho, A. Ebihara, S. Yokoyama, S. Kuramitsu, A. Shinkai, *Proteins Struct. Funct. Bioinf.* **2008**, *70*, 1108–1111.
[14] J. Jia, V. V. Lunin, V. Sauve, L. W. Huang, A. Matte, M. Cygler, *Proteins Struct. Funct. Genet.* **2002**, *49*, 139–141.
[15] M. Teplova, V. Tereshko, R. Sanishvili, A. Joachimiak, T. Bushueva, W. F. Anderson, M. Egli, *Protein Sci.* **2000**, *9*, 2557–2566.
[16] A. Pingoud, M. Fuxreiter, V. Pingoud, W. Wende, *Cell. Mol. Life Sci.* **2005**, *62*, 685–707.
[17] J. K. Frederiksen, J. A. Piccirilli, *Methods* **2009**, *49*, 148–166.
[18] H. Yonus, P. Neumann, S. Zimmermann, J. J. May, M. A. Marahiel, M. T. Stubbs, *J. Biol. Chem.* **2008**, *283*, 32484–32491.
[19] S. Schmelz, J. H. Naismith, *Curr. Opin. Struct. Biol.* **2009**, *19*, 666–671.
[20] A. Paschos, A. Bauer, A. Zimmermann, E. Zehelein, A. Bock, *J. Biol. Chem.* **2002**, *277*, 49945–49951.

[21] L. Forzi, R. G. Sawers, *Biometals* **2007**, *20*, 565 – 578.
[22] M. R. Leach, D. B. Zamble, *Curr. Opin. Chem. Biol.* **2007**, *11*, 159 – 165.
[23] P. M. Vignais, B. Billoud, J. Meyer, *FEMS Microbiol. Rev.* **2001**, *25*, 455 – 501.
[24] M. Blokesch, A. Paschos, A. Bauer, S. Reissmann, N. Drapal, A. Bock, *Eur. J. Biochem.* **2004**, *271*, 3428 – 3436.
[25] S. Reissmann, E. Hochleitner, H. F. Wang, A. Paschos, F. Lottspeich, R. S. Glass, A. Bock, *Science* **2003**, *299*, 1067 – 1070.
[26] B. El Yacoubi et al., *Nucleic Acids Res.* **2009**, *37*, 2894 – 2909.
[27] B. El Yacoubi, I. Hatin, C. Deutsch, T. Kahveci, J. P. Rousset, D. Iwata-Reuyl, G. Murzin, V. Crecy-Lagard, *EMBO J.* **2011**, *30*, 882 – 893.
[28] M. Srinivasan, P. Mehta, Y. Yu, E. Prugar, E. V. Koonin, A. W. Karzai, R. Sternglanz, *EMBO J.* **2011**, *30*, 873 – 881.
[29] E. M. Gustilo, A. P. F. Franck, P. F. Agris, *Curr. Opin. Microbiol.* **2008**, *11*, 134 – 140.
[30] F. V. Murphy, V. Ramakrishnan, A. Malkiewicz, P. F. Agris, *Nat. Struct. Mol. Biol.* **2004**, *11*, 1186 – 1191.
[31] M. Kuratani, T. Kasai, R. Akasaka, K. Higashijima, T. Terada, T. Kigawa, A. Shinkai, Y. Bessho, S. Yokoyama, *Proteins Struct. Funct. Bioinf.* **2011**, *79*, 2065 – 2075.
[32] B. N. Elkins, E. B. Keller, *Biochemistry* **1974**, *13*, 4622 – 4628.
[33] A. Körner, D. Soll, *FEBS Lett.* **1974**, *39*, 301 – 306.

